IEEE Access
Multidisciplinary | Rapid Review | Open Access Journal

SPECIAL SECTION ON MISSION CRITICAL SENSORS AND SENSOR NETWORKS (MC-SSN)

Received April 5, 2018, accepted May 23, 2018, date of publication May 29, 2018, date of current version June 20, 2018.

Digital Object Identifier 10.1109/ACCESS.2018.2841900

An EMD Based Sense-Through-Foliage Target Detection UWB Radar Sensor Networks

GANLIN ZHAO[1], QILIAN LIANG[1], (Fellow, IEEE), AND TARIQ S. DURRANI[2], (Fellow, IEEE)
[1]Department of Electrical Engineering, University of Texas at Arlington, Arlington, TX, 76019, USA
[2]Department of Electronic and Electrical Engineering, University of Strathclyde, Glasgow G1 1XQ, U.K.

Corresponding author: Ganlin Zhao (ganlin.zhao@mavs.uta.edu)

This work was supported in part by NSFC under Grants 61731006, 61771342, and 61711530132, in part by the Royal Society of Edinburgh, and in part by the Tianjin Higher Education Creative Team Funds Program.

ABSTRACT In this paper, we propose an empirical mode decomposition (EMD)-based approach to ultra wide band radar for sense-through-foliage target detection. When the radar signal quality is good, the EMD-based target detection approach performs well by comparing to the no target case. When the radar signal quality is poor and a single radar echo fails to detect the target, we first apply Rake structure in radar sensor networks to combine radar echoes from different radar cluster-members and then the EMD-based method could successfully carry out the target detection.

INDEX TERMS Target detection, foliage, radar sensor networks, EMD, UWB.

I. INTRODUCTION

Target detection and identification in a strong background clutter are significant topics of civilian and military research and applications. For example, in modern warfare, forest provides good cover for enemy military targets such as tanks, artillery and other weapon caches. Therefore, sense-through-foliage target detection is important for eliminating potential hostile enemy activities. However, the non-stationary nature of foliage environment, for example, doppler shift caused by tree leaves and branches blowing in the wind makes the target detection difficult. Despite of the dynamic and impulsive nature of background foliage clutter, it is also shown to be a rich scattering environment that multi-path propagation effects could dominate received echoes containing both target and clutter information [1].

In this paper, our goal is to make the target appear from the background foliage clutter based on our knowledge in signal processing and sensor networks using UWB radar. Compared to other types of signals used on foliage target detection study, such as waveforms used in UHF and VHF bands [2] to analyze attenuation and backscatter statistics of foliage and Millimeter-Wave radar [3], [4] used to detect target underneath foliage-cover, UWB radar operates at a relatively lower frequency band between 100MHz and 3GHz with a large fractional bandwidth greater than 20 percent. With such characteristics UWB radar is more suited for short distance application. However, the good penetration ability also high range resolutions make UWB radar has more advantage than narrow band signals in terms of target detection. In [5], radar channel modeling is studied using both UWB and narrowband measured radar sensor data in foliage environment.

Some previous works related to foliage penetration experiments using UWB radar have been conducted. In [6], DCT based approach is proposed to detect target through foliage. Reference [7] proposed differential and STFT based sense-through-foliage approaches. Meanwhile, some information theory based methods using mutual information [8], relative entropy [9] and multi-step information fusion [10] are applied on this topic. In [11], detection of man-made target obscured by foliage via UWB SAR imagery is studied. Also some theocratical works of opportunistic sensing and signal waveform design in radar sensor networks based on sense through foliage data are reported in [12] and [13]. Due to the characteristic of foliage which makes it difficult to use conventional time-frequency analysis to extract features of radar echoes, we are inspired by Empirical Mode Decomposition (EMD) for its ability to analyze nonlinear and non-stationary signals. EMD decomposes multi-component signals into several frequency components know as intrinsic mode functions (IMFs) and a residue(e.g. trend function with no frequency content) through a sifting process [14]. Some research works have employed EMD method to analyze radar target signal corrupted by sea clutter [15]. In [16] and [17], EMD based methods are also applied to sense through wall human target detection which could be treated as an oppo-

site scenario of sense-through-foliage since the human target has micro doppler shift caused by breadth and heart beat while the background clutter (wall) is stationary. In [18], a license plate localization method is proposed based on EMD analysis. In [19] EMD is shown to act as a dyadic filter bank in stochastic situations involving broadband noise. Also, bi-dimensional EMD(BEMD) is also widely used for image texture analysis and classification [20]–[22] as well as image target detection.

The rest of this paper is organized as follows: In Section II, we introduce the measurement and data collection used in the paper. In Section III, we present the background knowledge of EMD and Hilbert Transformation. In Section IV, we propose the EMD based sense-through-foliage target detection approach with good signal quality. In Section V, the combined RAKE structure and EMD based sense-through-foliage target detection is discussed when the signal has poor quality. In Section VI, we draw the conclusion.

II. DATA MEASUREMENT AND COLLECTION SETTINGS

In this work, the sense-through foliage data are provided by Air Force Research Lab [23]. The foliage penetration measurement effort began in late summer and continued through early winter. Late summer foliage involved in the measurement has decreased water content due to the limited rainfall. In this paper, the data we used involves defoliated foliage measured in late fall and winter.

The data collection experiment was conducted on a man lift. The total lifting capacity of the platform is 450 kg. The major equipment components are: Barth pulse generator, two antennas with mounting stand, Tektronix oscilloscope, RF switch, Signal generator and power supply. A model 732 GL Barth pulse source was used during the measurement. Coaxial reed switch is used by the pulse generator to generate less than 50 ps rise time pulses. The provided pulses also have amplitude from 150 V to greater than 2 KV into any load impedance through a 50 ohm coaxial line. The minimum width of produced pulses is 750 ps and the maximum width is up to 1 μs determined by capacitors or charge line length. The target is a trihedral shape metal reflector placed at 300 ft distance from UWB radar antennas as show in Figure 1.

For the data used in this paper, each data collection contains 16,000 samples. The total sample duration is 0.8 μs. 50 ps sample interval is used and approximate sample rate is 20 Hertz. We consider two different data sets from this measurement. Firstly, the pulse generator used low amplitude transmitting pulses to collect data. 35 reflected radar signals were averaged to produce each collection. One important property noted of these collections is that variability from different signal pulses was significant. We refer this collection as ''poor'' quality signal. Later, higher amplitude transmitting pulses are used for another data collection. Similarly, 100 reflected radar signals were averaged to produce each collection. We refer this collection as ''good'' quality signal.

FIGURE 1. A trihedral metal target placed at 300 feet from the lift.

III. EMPIRICAL MODE DECOMPOSITION AND HILBERT TRANSFORM

Empirical Mode Decomposition is introduced as part of Hilbert-Huang Transform (HHT) for non-stationary and nonlinear signal time-frequency analysis [24]. The main idea of EMD is to decompose the given multi-component signal into a series of finite intrinsic oscillatory basic functions and a residue through a ''sifting" process. These mono-component basic functions are called intrinsic mode functions (IMFs) represent different frequency components of the original signal and they satisfy two conditions: (1) the number of zero crossings and the number of local maximum or local minimum are either equal or differ at most by one; (2) the mean value of the envelope defined by the local maxima and the envelope defined by the local minima is zero at all points [24].

Compared to other time-frequency analysis methods, for example, wavelet transform and Short-Time Fourier Transform (STFT), the EMD algorithm is not only a fully data-driven but also adaptive method. The selection of window size of STFT is usually a tradeoff between time resolution and frequency resolution. Without a priori knowledge of suitable window size for certain applications, STFT can have performance degradation. The wavelet transform performance is greatly affected by the types of basic wavelet function employed [25]. Unlike these methods, the EMD does not require a priori basis functions and extracted basic functions from the data itself. The sifting process used in EMD of a given signal $x(t)$ is described as follows:

1) Identify all the local maxima and minima of $x(t)$.
2) Interpolate the local maxima using cubic spline line to obtain the upper envelope denote as $e_{upper}(t)$. Repeat the same procedure for local minima to obtain the lower envelope $e_{lower}(t)$.
3) Calculate the mean of upper and lower envelope $m_1(t) = (e_{upper}(t) - e_{lower}(t))/2$.
4) Calculate the difference between $x(t)$ and $m_1(t)$ as $h_1(t) = x(t) - m_1(t)$
5) Examine if $h_1(t)$ satisfy the two criteria of IMF. If it does not treat $h_1(t)$ as the original signal $x(t)$ and repeat

step1 - step4. Denote the the mean of upper and lower envelopes constructed from the extrema from $h_1(t)$ as $m_{11}(t)$. Then the difference between $h_1(t)$ and $m_{11}(t)$ is given as $h_{11}(t) = h_1(t) - m_{11}(t)$. Repeat this process k times until $h_{1k}(t) = h_{1(k-1)} - m_{1k}(t)$ meets the IMF criteria. Then the first IMF is extracted from the signal and designated as $c_1(t) = h_{1k}(t)$. However, to guarantee the extracted IMFs has enough physical meaning, a Cauchy type stop criterion is introduced to stop the sifting process if the standard deviation of two consecutive sifting output is less than a predefined value [26]:

$$SD = \sum_{t=0}^{T} \left[\frac{|h_{1(k-1)}(t) - h_{1k}(t)|^2}{h_{1(k-1)}^2(t)} \right] \tag{1}$$

SD value is usually between 0.2 and 0.3 [24].

6) Subtract $c_1(t)$ from the the rest of signal $x(t)$, the residue $r_1(t) = x(t) - c_1(t)$ is treated as signal $x(t)$ and repeat step1 - step5 n times to extract the rest IMFs from $c_2(t)$ to $c_n(t)$.

$$r_2(t) = r_1(t) - c_2(t)$$
$$\ldots$$
$$\ldots$$
$$r_n(t) = r_{n-1}(t) - c_n(t)$$

The sifting process ends until no IMF can be obtained from the residue $r_n(t)$ which means that $r_n(t)$ becomes a monotonic function. Therefore the original signals can be represented by all the extracted IMFs and the residue as:

$$x(t) = \sum_{i=1}^{n} c_j(t) + r_n(t) \tag{2}$$

Since the extracted intrinsic mode functions can be seen as monocomponent signals, it is straightforward to compute the Hilbert transform for each IMF to construct analytical signal which has meaningful instantaneous frequency. Let $\hat{c}_j(t)$ denotes the complex conjugate of the real valued signal $c_j(t)$:

$$\hat{c}_j(t) = \mathcal{H}[x(t)] = p.v.\frac{1}{\pi}\int_{\infty}^{-\infty} \frac{x(\tau)}{t-\tau} d\tau, \tag{3}$$

Where $p.v.$ indicates the Cauchy principal value. The analytical signal obtained from each IMF is then defined as:

$$s_j(t) = c_j(t) + i\hat{c}_j(t) = a_j(t)e^{i\theta_j(t)}, \tag{4}$$

where

$$a_j(t) = \sqrt{c_j^2 + \hat{c}_j^2}, \tag{5}$$

$$\psi_j(t) = arctan(\frac{\hat{c}_j}{c_j}). \tag{6}$$

$a_j(t)$ is the instantaneous amplitude and $\psi_j(t)$ is the phase of the analytical signal. The instantaneous frequency is:

$$\omega_j(t) = \frac{d\psi_j(t)}{dt} \tag{7}$$

After performing the Hilbert transform for each IMF component, Then we are able to calculate the Hilbert spectrum as the following:

$$\mathcal{H}(\omega, t) = \Re\left\{ \sum_{j=1}^{n} a_j(t) e^{[i\int \omega_j(t)dt]} \right\} \tag{8}$$

IV. SENSE-THROUGH-FOLIAGE TARGET DETECTION WITH GOOD QUALITY SIGNAL USING EMD APPROACH

In Figure 2, we plot two collections of data with good signal quality. Figure 2(a) shows the received echoes without target on range. Figure 2(b) shows the received echoes with target's presence around 14,000 sample. For a more clear view, we expand views of Figure 2 from sample 13,001 to 15,000 as plotted in Figure 3(a) without target and Figure 3(b) with target respectively. Since the Figure 3(a) has no target on range, it can be treated as the pure background clutter response. Therefore, it is intuitive to calculate the echo difference between Figure 3(a) and Figure 3(b) and the result is shown in Figure 3(c). From Figure 3(c) we can observe that target appears at around sample 14,000. However, practically it is impossible for us to obtain both collections of data (Figure 3(a) and Figure 3(b)) simultaneously. We can

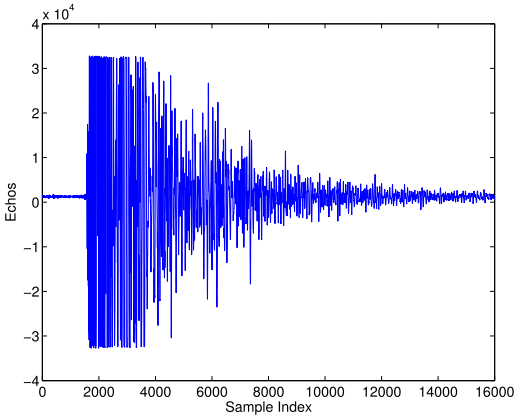

(a)

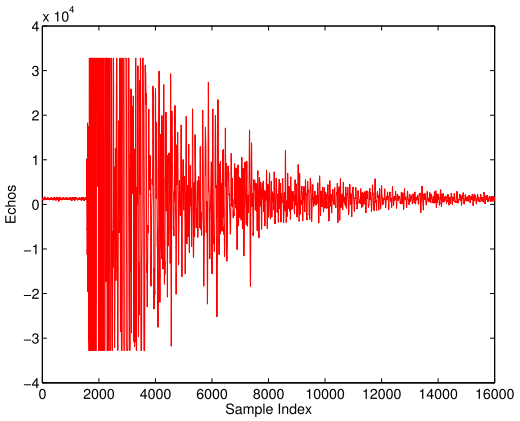

(b)

FIGURE 2. Good quality signal measurement. (a) Without target (b) Target on range.

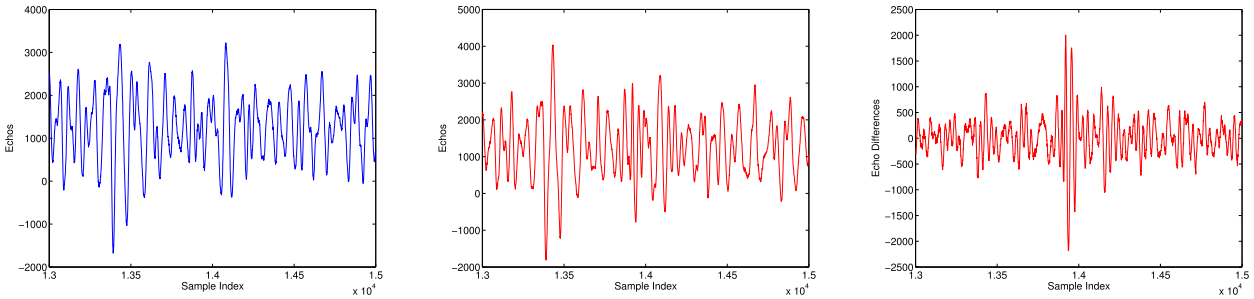

(a) (b) (c)

FIGURE 3. Expanded view of a good quality signal measurement from samples 13,001 to 15,000. (a) Without target. (b) Target on range at around 14,000 sample. (c) Differences between echoes in (a) and echoes in (b).

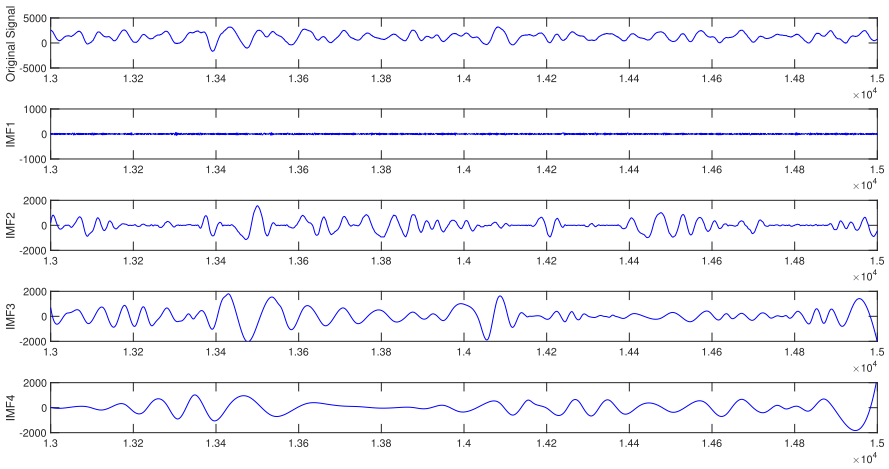

(a)

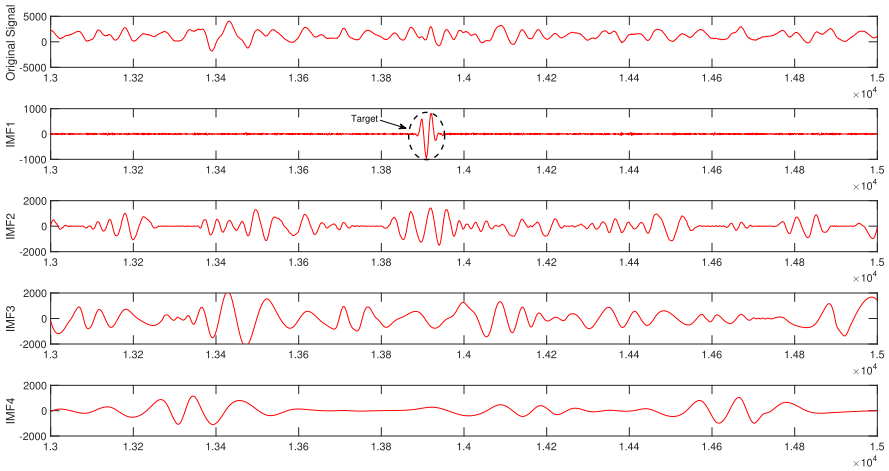

(b)

FIGURE 4. EMD results with good signal quality. (a) Original signal and IMF1-4 with no target on range, (b) Original signal and IMF1-4 with target on range (Observed target signature in IMF1 at around sample 13,900).

only detect target based on one of them(Figure 3(a) or Figure 3(b)).

V. SENSE-THROUGH-FOLIAGE TARGET DETECTION WITH POOR QUALITY SIGNAL USING RSN AND EMD APPROACH

The real world data usually tends to be non-stationary in nature. Motivated by this, we apply the EMD algorithm to our two collections of data to see if any useful information about the target can be extracted. Since the EMD is an iterative algorithm which is time consuming, in this paper, by comparing the results obtained using different stopping criteria, we confine the each sifting process to 11 iterations and the obtained result is good enough to conduct target detection task. After applying EMD for samples provided in Figure 3(a) and Figure 3(b), we plot the first four order

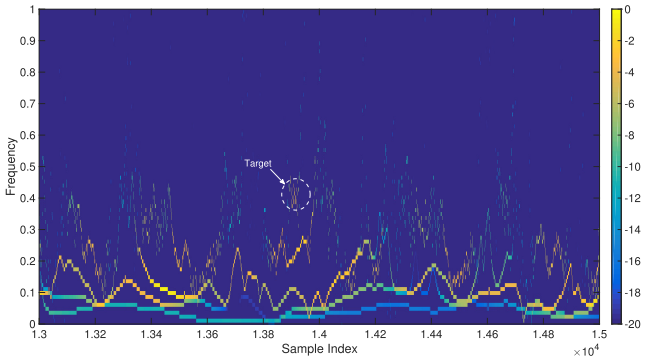

FIGURE 5. Hilbert spectrum of original signal.

IMFs extracted from the sifting process in Figure 4. Observed from Figure 4(b) which is the EMD result of echoes with target, the first IMF which contains the highest frequency component of original signal has a higher amplitude oscillation at around sample 14,000 compared to other sample locations. Due to the fact that the foliage clutter is very impulsive and behaves like Gaussian distributed noise [6] in the frequency domain, it is impossible to separate target and noise in each IMF which means each IMF contains both information about target and foliage clutter. However, in the first IMF sample locations other than sample around 14,000 have low amplitude fluctuations and behave like Gaussian noise. We can conclude that the high energy oscillation around sample 14,000 in IMF1 is the signature of the target and this also imply higher signal to clutter ratio (SCR) in high frequency. We also plot the IMFs extracted from the signal without target as shown in Figure 4(a) that in the first IMF we don't notice any obvious change in all sample locations and it can represent the foliage clutter feature. This also proves our conclusion by comparing the two figures. Figure 5 is the Hilbert Spectrum of the original signal.

As mentioned in Section II, when the Barth pulse generator was operated at low amplitude, only 35 pulses are averaged for each collection. This results in poor return signal quality since not enough pulse averaging are used to obtain the sample value. We plot the two collections of data with poor signal quality in Figure 6(a) without target, Figure 6(b) with target on range and Figure 6(c) the difference between two data collections. From Figure 6(c) we are not able to tell whether there's a target. Also, in Figure 7(a) and Figure 7(b) we draw the extracted IMFs results using EMD approach from these two data collections. From the high frequency IMFs we are not able to observe any noticeable target signature. Experiments also validate that applying EMD to each single collection of poor quality signal fails to detect the target. However, significant pulse-to-pulse variability is observed in the UWB radar receive echoes. Assuming measurements are independent, we are motivated to explore some diversity combining techniques in Radar Sensor Networks (RSN) to improve the received signal quality.

In this case, we propose to use a RAKE structure to handle poor signal quality target detection problem. RAKE structure is an effective diversity combining method due to the fact that uncorrelated radar measurements could experience different fading levels. Echoes from different cluster-member radars are combined by the cluster head. We consider two different diversity combing schemes to implement Rake structures: equal gain combing and maximum ratio combining. The equal gain combined signal can be formulated as the following:

$$x_{eq}(n) = \frac{1}{M}\sum_{i=1}^{M} x_i(n). \tag{9}$$

Here M is the number of radar echoes used in the combining.

The maximum ratio combing scheme uses a weighted average w_i determined by the power of each echo $x_i(n)$ (n is the sample index),

$$E_i = \mathrm{var}(x_i(n)) + [\mathrm{mean}(x_i(n))]^2, \tag{10}$$

where

$$w_i = \frac{E_i}{\sum_{i=1}^{M} E_i}. \tag{11}$$

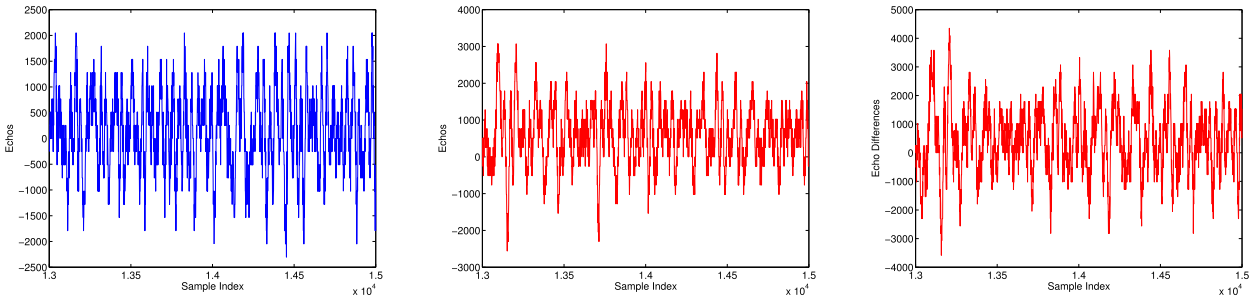

FIGURE 6. Expanded view of a poor quality signal measurement from samples 13,001 to 15,000. (a) Without target. (b) Target on range at around 14,000 sample. (c) Differences between echoes in (a) and echoes in (b).

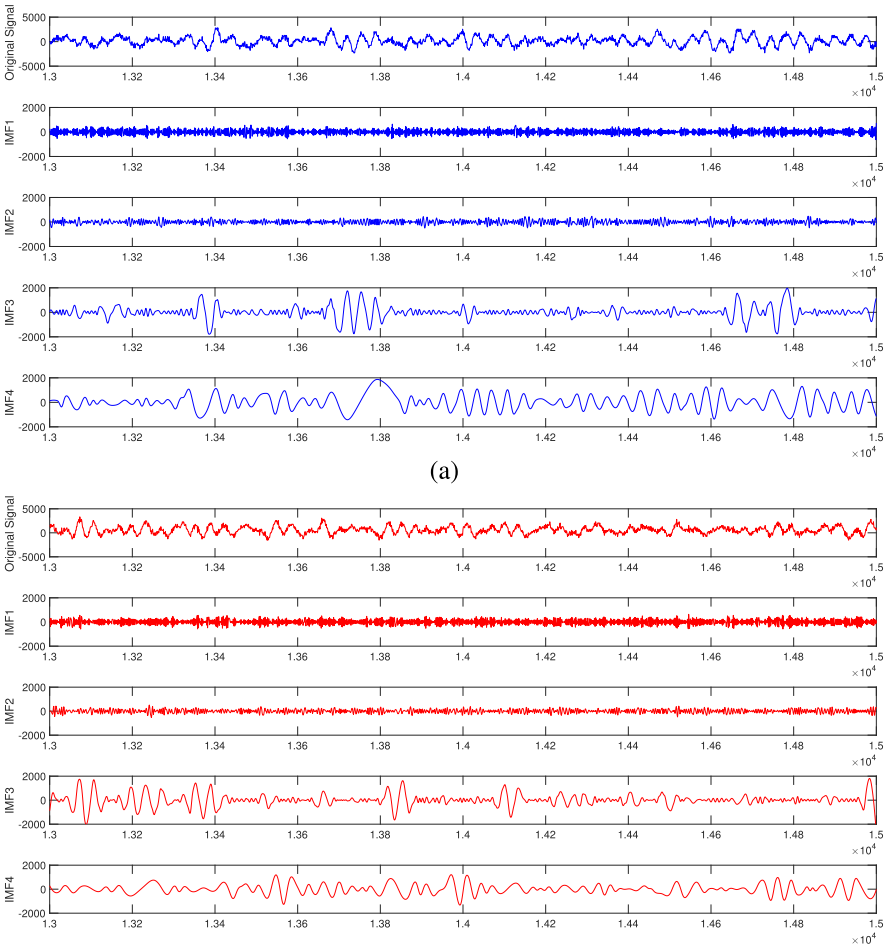

FIGURE 7. EMD results with poor signal quality. (a) Original signal and IMF1-4 with no target on range, (b) Original signal and IMF1-4 with target on range.

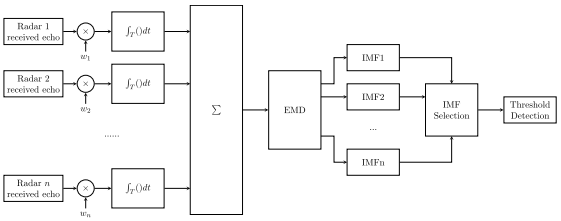

FIGURE 8. Block diagram of RAKE struture.

The maximum ratio combined signal has following form:

$$x_{mrc}(n) = \sum_{i=1}^{M} w_i x_i(n) \tag{12}$$

After the diversity combing EMD is applied to the combined signal. We plot the IMFs extracted from two cases in Figure 9(a) (without target) and Figure 9(b) (with target). In Figure 9(b), from first IMF with highest frequency component, we cannot tell if there's a target. However, in the second IMF with second highest frequency, we observe a high amplitude oscillation around sample 14,000. Also in Figure 9(a) which represents the IMFs of foliage clutter and we do not observe anything in the first two IMFs. Therefore, we conclude this high amplitude oscillation in IMF2 is the target signature. This observation is also in accordance with the result of target detection of good quality signal.

In our database, totally 70 radar echoes can be used to construct the Rake structure receiver. We further investigate the RAKE structure performance at different combing levels. For example, we randomly choose $M = 10$, $M = 20$ and $M = 30$ radar echoes in the database and 10,000 Monte Carlo simulations are performed at each combing level. Figure 10 shows the probability of detection with different thresholds for equal gain combing and maximum ration combing schemes. From the figure we can see that the maximum ratio combing method outperforms equal gain combing method at each combing level. Using more radars also improves the detection accuracy.

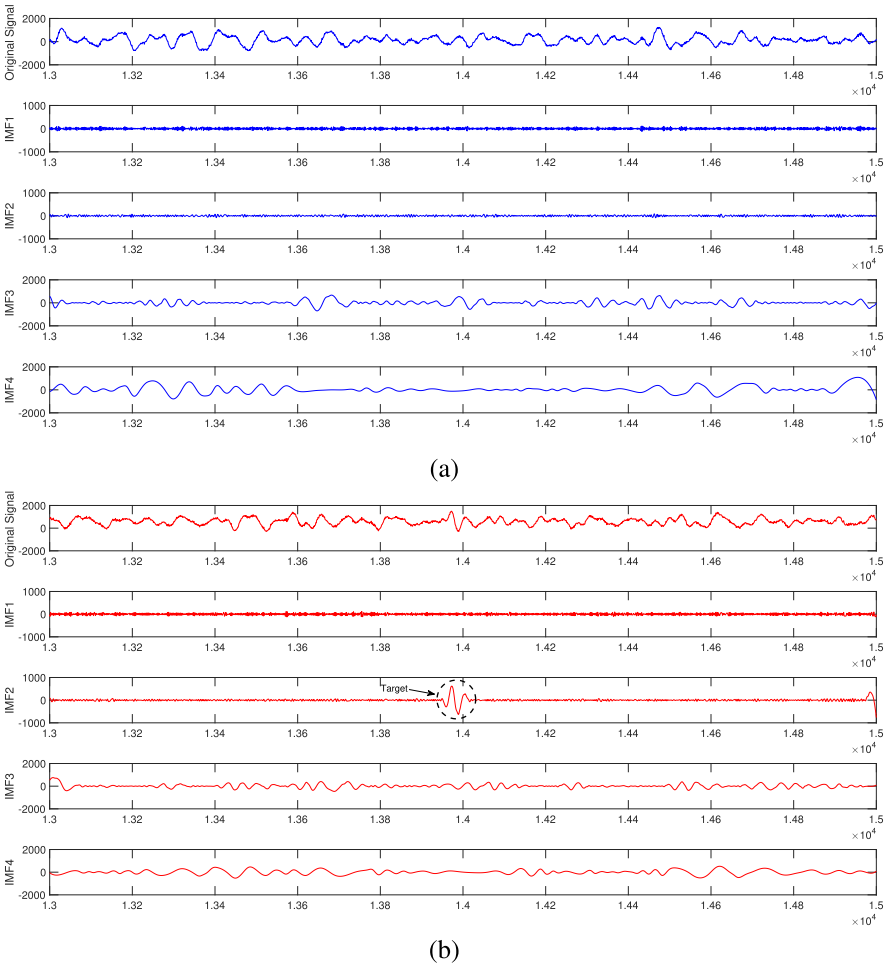

FIGURE 9. EMD results with poor signal quality after RAKE structure combing. (a) Original signal and IMF1-4 with no target on range, (b) Original signal and IMF1-4 with target on range. (Observed target signature in IMF2 at around sample 14,000).

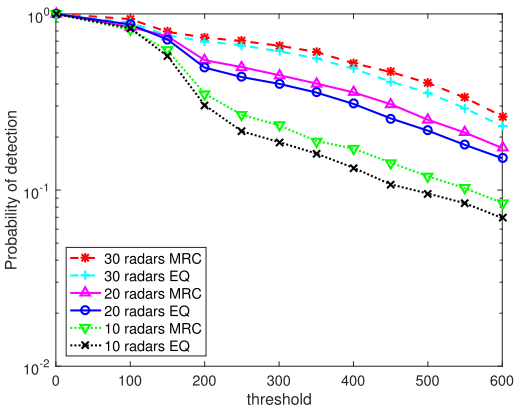

FIGURE 10. Probability of detection using maximum ratio combing and equal gain combing at radar combing level $M = 10$,$M = 20$ and $M = 30$.

VI. CONCLUSION

An EMD based approach for sense-through-foliage target detection is studied. After extracted IMFs from the original signal through sifting process, we are able to observe target signature in the first IMF which represents the highest frequency component when the signal quality is good. When the signal quality is poor and a single collection of radar echo cannot carryout target detection, a RAKE structure in RSN using cluster-head radar by combining echoes from different cluster-member radars is used for preprocessing before applying EMD algorithm. From the second extracted IMF we are able to find similar target signature as the one appears in good quality signal. Simulation results indicate that using more combined radar echoes improves the detection accuracy.

REFERENCES

[1] J. Liang, Q. Liang, and S. W. Samn, "Foliage clutter modeling using the UWB radar," in *Proc. IEEE Int. Conf. Commun.*, Beijing, May 2008, pp. 1937–1941.

[2] S. Ayasli and L. Bessette, "UHF & VHF SAR phenomenology," presented at the Proc. PIERS, Workshop Adv. Radar Methods, Baveno, Italy, Jul. 1998.

[3] A. Y. Nashashibi, K. Sarabandi, S. Oveisgharan, M. C. Dobson, W. S. Walker, and E. Burke, "Millimeter-wave measurements of foliage attenuation and ground reflectivity of tree stands at nadir incidence," *IEEE Trans. Antennas Propag.*, vol. 52, no. 5, pp. 1211–1222, May 2004.

[4] A. Y. Nashashibi and F. T. Ulaby, "Detection of stationary foliage-obscured targets by polarimetric millimeter-wave Radar," *IEEE Trans. Geosci. Remote Sens.*, vol. 43, no. 1, pp. 13–23, Jan. 2005.

[5] Q. L. Liang, "Radar sensor wireless channel modeling in foliage environment: UWB versus narrowband," *IEEE Sensors J.*, vol. 11, no. 6, pp. 1448–1457, Jun. 2011.

[6] Q. Liang, S. W. Samn, and X. Cheng, "UWB radar sensor networks for sense-through-foliage target detection," in *Proc. IEEE Int. Conf. Commun.*, Beijing, May 2008, pp. 2228–2232.

[7] J. Liang and Q. Liang, "Sense-through-foliage target detection using UWB radar sensor networks," *Pattern Recognit. Lett.*, vol. 31, no. 11, pp. 1412–1421, 2010.

[8] I. Maherin and Q. Liang, "A mutual information based approach for target detection through foliage using UWB radar," in *Proc. IEEE Int. Conf. Commun. (ICC)*, Ottawa, ON, Canada, Jun. 2012, pp. 6406–6410.

[9] I. Maherin and Q. Liang, "Radar sensor network for target detection using Chernoff information and relative entropy," *Phys. Commun.*, vol. 13, pp. 244–252, Dec. 2014.

[10] I. Maherin and Q. Liang, "Multi-step information fusion for target detection using UWB radar sensor network," *IEEE Sensors J.*, vol. 15, no. 10, pp. 5927–5937, Oct. 2015.

[11] R. Kapoor and N. Nandhakumar, "Features for detecting obscured objects in ultra-wideband (UWB) SAR imagery using a phenomenological approach," *Pattern Recognit.*, vol. 29, no. 11, pp. 1761–1774, 1996.

[12] Q. Liang, X. Cheng, S. C. Huang, and D. Chen, "Opportunistic sensing in wireless sensor networks: Theory and application," *IEEE Trans. Comput.*, vol. 63, no. 8, pp. 2002–2010, Aug. 2014.

[13] Q. Liang, X. Cheng, and S. W. Samn, "NEW: Network-enabled electronic warfare for target recognition," *IEEE Trans. Aerosp. Electron. Syst.*, vol. 46, no. 2, pp. 558–568, Apr. 2010.

[14] Z. Wu and N. E. Huang, "Ensemble empirical mode decomposition: A noise-assisted data analysis method," *Adv. Adapt. Data Anal.*, vol. 1, no. 1, pp. 1–41, 2008.

[15] J. Guan, J. Zhang, N. Liu, and B. Li, "Time-frequency entropy of Hilbert-Huang transformation for detecting weak target in sea clutter," in *Proc. IEEE Radar Conf.*, Pasadena, CA, USA, May 2009, pp. 1–5.

[16] P.-H. Chen, M. C. Shastry, C.-P. Lai, and R. M. Narayanan, "A portable real-time digital noise radar system for through-the-wall imaging," *IEEE Trans. Geosci. Remote Sens.*, vol. 50, no. 10, pp. 4123–4134, Oct. 2012.

[17] J. Li, L. Liu, Z. Zeng, and F. Liu, "Advanced signal processing for vital sign extraction with applications in UWB radar detection of trapped victims in complex environments," *IEEE J. Sel. Topics Appl. Earth Observat. Remote Sens.*, vol. 7, no. 3, pp. 783–791, Mar. 2014.

[18] S. Yu, B. Li, Q. Zhang, C. Liu, and M. Q.-H. Meng, "A novel license plate location method based on wavelet transform and EMD analysis," *Pattern Recognit.*, vol. 48, no. 1, pp. 114–125, 2015.

[19] P. Flandrin, G. Rilling, and P. Goncalves, "Empirical mode decomposition as a filter bank," *IEEE Signal Process. Lett.*, vol. 11, no. 2, pp. 112–114, Feb. 2004.

[20] J. C. Nunes, S. Guyot, and E. Deléchelle, "Texture analysis based on local analysis of the bidimensional empirical mode decomposition," *Mach. Vis. Appl.*, vol. 16, no. 3, pp. 177–188, 2005.

[21] X. Guanlei, W. Xiaotong, and X. Xiaogang, "Improved bi-dimensional EMD and Hilbert spectrum for the analysis of textures," *Pattern Recognit.*, vol. 42, no. 5, pp. 718–734, 2009.

[22] X. Guanlei, W. Xiaotong, and X. Xiaogang, "On analysis of bi-dimensional component decomposition via BEMD," *Pattern Recognit.*, vol. 45, no. 4, pp. 1617–1626, 2012.

[23] C. Dill, "Foliage penetration (Phase II) field test: Narrowband versus wideband foliage penetration," Final Rep. F41624-03, Jul. 2005.

[24] N. E. Huang *et al.*, "The empirical mode decomposition and the Hilbert spectrum for nonlinear and non-stationary time series analysis," *Proc. Roy. Soc. London A, Math., Phys. Eng. Sci.*, vol. 454, no. 1971, pp. 903–995, Mar. 1998.

[25] I. Daubechies, "The wavelet transform, time-frequency localization and signal analysis," *IEEE Trans. Inf. Theory*, vol. 36, no. 5, pp. 961–1005, Sep. 1990.

[26] G. Wang *et al.*, "On intrinsic mode function," *Adv. Adapt. Data Anal.*, vol. 2, no. 3, pp. 277–293, 2010.

GANLIN ZHAO received the B.S. degree from Tianjin University in 2012, the M.S. degree from the University of Rochester in 2014, and the Ph.D. degree from the University of Texas at Arlington in 2017, all in electrical engineering. His research interests include wireless communications, signal processing, radar sensor networks, UWB, radar target detection, wireless sensor networks, and MIMO. He received the Research in Motion Outstanding Graduate Scholarship Award in 2016.

QILIAN LIANG (F'01) received the Ph.D. degree in electrical engineering from the University of Southern California in 2000. He was a member of Technical Staff with Hughes Network Systems Inc., San Diego, CA, USA. He is currently a Distinguished University Professor with the Department of Electrical Engineering, University of Texas at Arlington (UTA). He has published over 300 journals and conference papers. His research interests include wireless sensor networks, wireless communications, signal processing, and computational intelligence. He received the 2002 IEEE TRANSACTIONS ON FUZZY SYSTEMS Outstanding Paper Award, the 2003 U.S. Office of Naval Research Young Investigator Award, the 2007, 2009, and 2010 U.S. Air Force Summer Faculty Fellowship Program Award, the 2012 UTA College of Engineering Excellence in Research Award, and the 2013 UTA Outstanding Research Achievement Award. He was inducted into the UTA Academy of Distinguished Scholars in 2015.

TARIQ S. DURRANI (F'89) was a University Deputy Principal with major responsibility for University-wide strategic developments in computing/information technology infra-structure, entrepreneurship, staff development, and lifelong learning, from 2000 to 2006. He joined the University of Strathclyde as a Lecturer in 1976, and became a Professor in 1982, and the Department Head from 1990 to 1994 of one of the largest U.K. EEE Departments. He was the Director of the U.K. Government DTI Centre for Parallel Signal Processing from1989 to 1991 and the U.K. Research Council/DTI Scottish Transputer Centre from 1991 to 1995 with the University of Strathclyde. He was the Chair with the Institute for Communications and Signal Processing from 2006 to 2007, and the Head of the Centre of excellence in Signal and Image Processing from 2008 to 2009. He is currently a Research Professor in electronic and electrical engineering with the University of Strathclyde. He has authored six books and over 350 publications. He has supervised over 40 Ph.D. theses. His research interests include communications, signal processing, technology management, and higher education management. He is a fellow of the Royal Academy of Engineering, the Royal Society of Edinburgh, and IET, and is a Foreign Member of the U.S. National Academy of Engineering. He has been a Vice President (Natural Sciences from 2007 to 2010), and is also a Vice President (International from 2012 to 2013) of the Royal Society of Edinburgh, National Academy of Scotland; Council (Board) Member of the Scottish Funding Council-which distributes $3.0 billion equivalent funding annually to universities and colleges.